Supplemental Tables

Supplemental Table 1. RNA-seq data for genes in ontology "muscle system process", “cell cycle” and “mitochondrion”.

Supplemental Table 2. Gene lists used in GO enrichment analysis.

Supplemental Table 3. Mitochondrial genes that are bound by both pRb and Kdm5a.

Supplemental Table 4. TFBS enriched in gene sets of interest (corrected right *P* value < 0.02).

Supplemental Table 5. List of primers.

Supplemental Figures

Supplemental Figure 1. Dependence of myogenic differentiation on pRb and Kdm5a. (*A*) Reintroduction of *Rb1* in $Rb1^{-/-}$ MEFs using lentiviral system rescues myogenic differentiation. Tamoxifen-inducible MyoD was introduced in $Rb1^{-/-}$ MEFs using MyoDER[T]. Next, cells were transduced with pLenti-FLAG-empty (“vector”) control or pLenti-FLAG-RB (“pRB”) and the medium was changed to DM with 100 nM 4-hydroxytamoxifen for 72 h. Cells were visualized using brightfield microscopy at 100x and 200x (2x ZOOM) magnification. (*B*) Detection of pRB expression in cells from **a** by immunoblotting with anti-FLAG or anti-RB antibodies. (*C*) $Rb1^{-/-}$ MEFs can be rescued for muscle gene expression, cell cycle arrest and multinucleation by reintroduction of pRB protein. Cells generated as in *A* were stained with anti-MyHC, EdU and DAPI. (*D*) Average percentage of EdU-positive cells + standard deviation (s.d.), $n = 5$ microscopic fields (20x objective). (*E*) Knockdown of *Rb1* inhibits myogenic differentiation and is rescued by the accompanying *Kdm5a* knockdown. C2C12 cells were transduced with *Rb1* and *Kdm5a* lentiviruses and induced for differentiation for 48 h. Control 1 is the control shRNA for *Rb1* shRNAs. Control 2 is the mixture of two shRNAs as a control for the mixture of *Rb1* and Kdm5a shRNAs. Cells were

stained with anti-MyHC and DAPI. (*F*) Quantification of MyHC-positive cells. Cells were counted in 10 microscopic fields (40x objective). Mean ± s.d. for $n = 2$ independent experiments. (*G*) Immunoblot analysis of cell lysates prepared from induced C2C12 cells that were transduced with controls, *Rb1* or *Kdm5a* shRNAs, as in E. (*H*) Size fractionation procedure to obtain a pure population of myotubes for RNA-seq experiment**.** MEFs were transduced with Adeno-MyoD and induced for differentiation for 72 h. Following trypsinization, small undifferentiated cells staying in suspension were removed by aspiration while the large myotubes promptly sedimented. For details, see Supplemental Materials and Methods. Microscopic images of DKO cells were taken before and after fractionation. Nuclei were stained with DAPI to examine proportion of multinucleated cells. Using this procedure, myotubes were successfully purified from a mixed population of undifferentiated and differentiated cells.

Supplemental Figure 2. DKO exhibits earlier induction of myogenic differentiation than the WT. (*A*) Fluorescent microscopy of myogenin (Myog) expression during the differentiation time course. WT, *Kdm5a*$^{-/-}$, *Rb1*$^{-/-}$, and DKO MEFs were induced to differentiate for 0, 6, 12, 18, 24, 36, 48 and 144 h. Cells were stained with anti-Myog antibody and counter stained with the nuclear stain DAPI. (*B*) Myog-positive cells were quantified and are represented as the percentage of the total cell number. (*C*) Quantitation of Myog-positive cells shown specifically at the 12-h time point. Means ± standard error of the mean (s.e.m.), $n = 3$ biological replicates. Student's *t* test was done to indicate the significant difference between the samples; *P* - values are indicated. (*D*) MyoD binding at the *Myog* region in differentiating C2C12 myoblasts from ENCODE/Caltech data. (*E*) MyoD is bound at the *Myog* promoter in induced for 24 h DKO but not *Rb1*$^{-/-}$ MEFs. Binding to the control *Igr2* region is shown. Means ± s.e.m., $n = 2$ biological replicates.

Supplemental Figure 3. Assays for cell cycle re-entry. (*A*) WT, *Kdm5a*$^{-/-}$, *Rb1*$^{-/-}$ and DKO MEFs were induced to differentiate in media containing 2% horse serum. Cells were then stimulated in high-serum media (20% FBS). EdU incorporation indicates S-phase entry; histone 3 serine 10 phosphorylation (H3S10p) is a marker of G2/M phase; these stains are used in conjunction with MyHC and DAPI stain. Images were generated using confocal microscope. (*B*) Quantitation of differentiated cells, marked by MyHC, that were positive for cell cycle reentry, marked by EdU or H3S10p, for each of the indicated genotypes. In the case of multinucleated cells, if multiple nuclei in the same cell were positive for EdU or H3S10p, the cell was counted only once. Data is shown as the percentage of EdU-positive myotubes or H3S10p-positive myotubes (means ± s.e.m., n = 3 biological replicates) out of the total cell number. (*C*) Loss of even a single copy of *Kdm5a* rescues MyHC expression but unable to rescue cell cycle progression. ICC was performed in parallel to the experiments in *A*.

Supplemental Figure 4. Developmental genes occupied by Kdm5a are not rescued in DKO. (*A*) Developmental genes occupied by Kdm5a are downregulated during myogenic differentiation. C2C12 cells were induced for 0, 24, 48 and 96 h. RT-qPCR data was normalized to *B2m* level and presented as Log_2 fold change relative to uninduced condition (0 h). Many Kdm5a targets that are differentiation markers are repressed after induction, along with cell cycle genes. In contrast, the myogenic markers that are highly upregulated during induction (on the *left*) are not Kdm5a targets. Mean $\pm$ s.e.m. for n = 3 RT-qPCR reactions. (*B*) Developmental genes occupied by Kdm5a are downregulated in induced MEFs. MEFs were transduced with Adeno-MyoD or with Adeno (null) viruses and induced to differentiate for 72 h. Expression level of myogenic markers, Kdm5a targets

(with Kdm5a location in a distal or proximal promoter region) with function in differentiation and Kdm5a targets with function in cell cycle was determined by RT-qPCR. Data were normalized to the *Gapdh* level and presented as Log_2 fold difference in Adeno-MyoD versus empty Adeno vector. Mean ± s.e.m. for $n = 2$ RT-qPCR reactions. Activation of myogenic markers in induced MEFs is comparable to the induced C2C12 myoblasts. (*C*) Developmental genes occupied by Kdm5a are expressed in myotubes at a relatively low level. The expression level for genes in *B* and in Fig. 2A relative to the median expression value was compared in DKO-myo and WT-myo using RNA-seq data.

Supplemental Figure 5. Rescue of mitochondrial genes and their products correlates during myogenic differentiation with the rescue of myogenic markers. (*A*) Expression level of representative myogenic markers. (*B*) Additional genes with mitochondrial function are shown to the data in Fig. 2C. Expression level of each gene was analyzed in four different genotypes at 0, 24 and 96 h after induction. All RT-qPCR data were normalized to spikes and is shown as fold change relative to WT at 0 h for each gene. Mean ± s.e.m. for $n = 3$ RT-qPCR replicates. (*C*) Protein level of mitofusin Mfn2 and the transcriptional co-activator Pgc-1α are progressively increased during differentiation of C2C12 cells. (*D*) Protein level of specific mitochondrial proteins encoded by Kdm5a target genes are rescued in DKO compared to $Rb1^{-/-}$ MEFs induced for 72 h, along with the gene encoding MyHC. In C and D, total cell extracts were loaded at the same relative amounts and immunoblot analysis was performed with the indicated antibodies, and with vinculin and α-tubulin as loading controls.

Supplemental Figure 6. *Kdm5a* loss rescues adipocyte differentiation in *Rb*-negative cells. (*A*) Induced MEFs show differences in lipid accumulation depending on *Rb1* status. MEFs were induced to differentiate for 72 and 120 h in adipogenic DM. Oil Red O staining was performed and visualized by light microscopy. (*B*) Quantitation of lipid accumulation. Oil Red O was extracted and quantified by measuring absorbance at 490 nm. Fold change differences in absorbance values, normalized to protein concentration, are shown relative to the undifferentiated WT (0 h) MEFs. Means + s.d., n = 3 replicate wells. (*C*) Activation of adipogenic markers in MEFs of different genotypes. MEFs were induced to differentiate for 24 and 96 h and compared to uninduced (0 h) WT MEFs. Expression of four Kdm5a targets with functions in the mitochondrion was analyzed at three time-points in the WT and at two time-points in other genotypes. RT-qPCR data is normalized to spike controls; mean $\pm$ s.e.m. for n = 3 biological replicates. (*D*) Activation of genes encoding mitochondrial components at early differentiation failed in *Rb1*$^{-/-}$ MEFs but may be partially restored in DKO back towards WT levels. Data was analyzed as in C.

Supplemental Figure 7. Expression of KDM5A in DKO MEFs using lentiviral system and larger images for other figures. (*A*) DKO cells were transduced with pLenti-FLAG-KDM5A wild-type or demethylase mutant. ICC was performed in transduced DKO cells and in WT cells as a control with anti-KDM5A antibody (green) or anti-FLAG (red) antibody and DAPI. (*B*) Enlarged images in Fig. 1B. (*C*) Enlarged images in Fig. 3B. (*D*) Enlarged images in Fig. 4A.

Supplemental Figure 8. Mitochondrial morphology and mitochondrial mass is rescued in DKO cells. (*A*) Four mitochondrial classes based on morphology. Mitochondria are highly dynamic organelles appearing in tubular networks, as large spheres or small rods. ICC staining for Cox IV

identified differences in mitochondrial shape that were used for classification. (*B*) Cox IV expression reveals that representative mitochondrial classes are similar in WT, *Kdm5a*$^{-/-}$ and DKO but different in *Rb1*$^{-/-}$ cells. ICC staining was performed for Cox IV and for MyHC, in order to identify myotubes. For more detail, each image was digitally zoomed to area indicated in the red box. (*C*) MitoTracker staining reveals that representative mitochondrial classes are similar in WT, *Kdm5a*$^{-/-}$ and DKO but different in *Rb1*$^{-/-}$ cells. For more detail, each image was digitally zoomed to area indicated in the yellow box. (*D*) Quantitation of mitochondrial morphology based on Cox IV staining. Morphology was quantified as the percentage of cells containing mitochondria that best fit a particular class. (*E*) Quantitation of mitochondrial morphology based on MitoTracker staining. All analyses were performed in proliferating MEFs and in MEFs transduced with Adeno-MyoD that were induced for 96 h; mean $\pm$ s.e.m. for $n = 2$ experiments (> 300 cells per experiment).

Supplemental Figure 9. (*A*) Kinetics of the ECAR response to acute addition of glucose, followed by injection of the inhibitor of respiration oligomycin and hexokinase inhibitor 2-DG to reveal contribution from glycolysis. MEFs of four genotypes were transduced with Lenti-empty vector (0 h) or with Lenti-MyoD and induced for 18 h. Assays were performed using XF^{e}96 Extracellular Flux Analyzer. Upon completion of an assay, cells were lysed and protein content was determined. Data was normalized to the protein content. (*B*) Glucose utilization in 0 h and 18 h-treated cells of different genotypes. The difference in OCR was measured acutely after glucose injection by comparing measurements 4 (after injection) and 3 (before injection). *** $P < 0.0001$ and ** $P < 0.01$ is shown for DKO relative to the *Rb1*$^{-/-}$. (*C*) Effect of metformin on palmitate-induced OCR in cells induced for differentiation. MEFs of four different genotypes were transduced as in A and induced along with C2C12 cells for 18 h. Pre-treatment with metformin was performed where indicated. Data

in B and C is presented as fold change relative to the 0 h WT MEFs. (*D*) WT MEFs are susceptible to the action of RCI inhibitors, as determined by increased phospho-ACC Ser79. Immunoblotting was performed using lysates from cells treated with rotenone, cells treated with metformin and phenformin in the range of mM concentrations, and untreated cells. (*E*) Quantitation of MyHC in induced MEFs treated with RCI inhibitors. Induced WT MEFs were stained for MyHC and cleaved caspases 3 and percent of positive cells was calculated. The level of apoptosis stays very low in cells treated with RCI inhibitors. No apoptotic induction was also observed with either using cleaved caspases 3 or *in situ* staining using CaspaACE FITC-VAD-FMK (data not shown). Mean ± s.d. for $n = 3$. (*F*) The RCI inhibitors phenformin and metformin block myogenic differentiation at high nanomolar concentrations. Representative confocal images are shown for ICC MyHC in cells treated the inhibitors or vehicle.

Supplemental Figure 10. Efficiency of KDM5A knockdown and level of Pgc-1α overexpression achieved in transduced *RB*-negative cell lines as determined by immunoblot analysis.

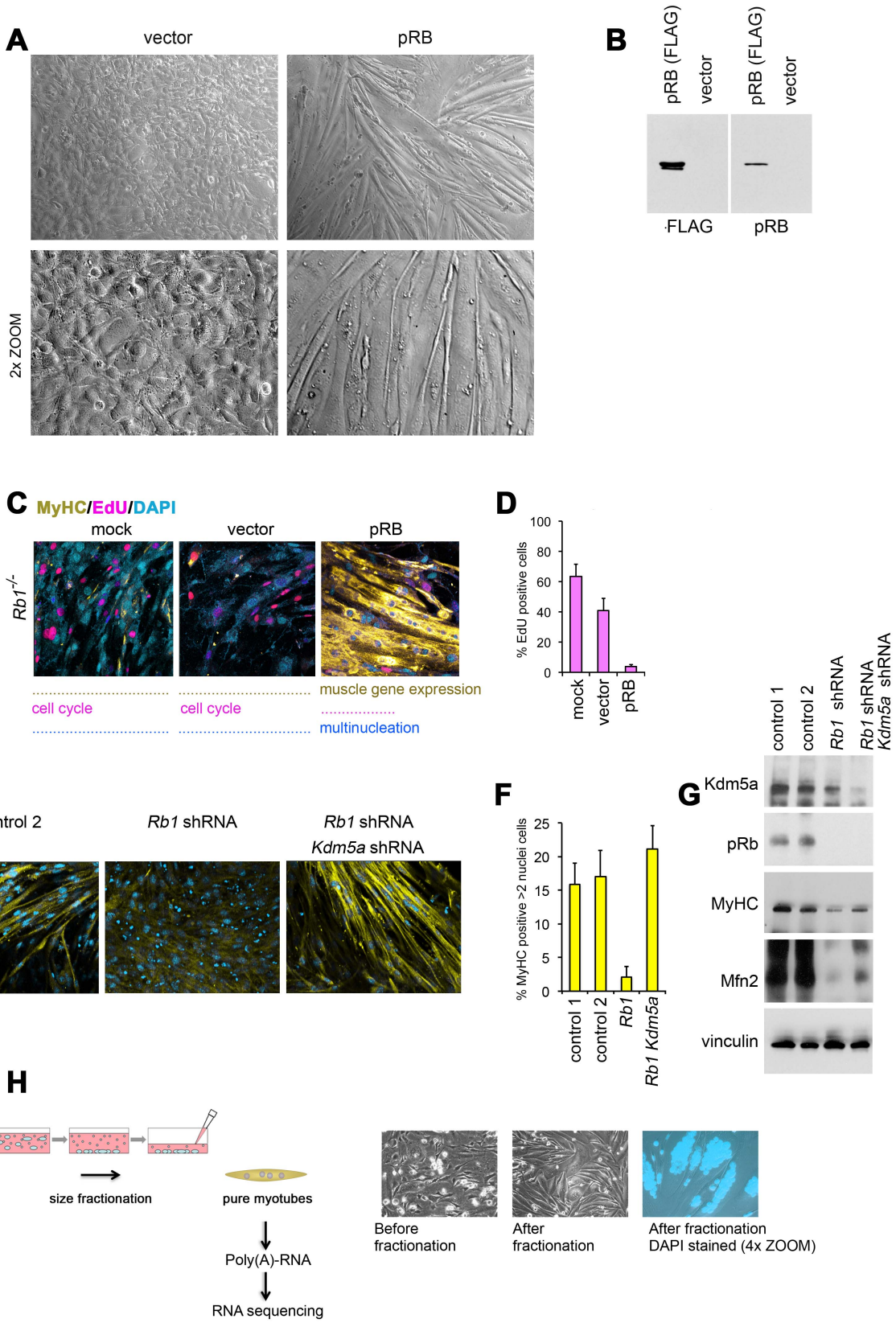
A
vector
pRB
2x ZOOM
B
pRB (FLAG)
vector
pRB (FLAG)
vector
FLAG
pRB
C
MyHC/EdU/DAPI
mock
vector
pRB
Rb1-/-
muscle gene expression
cell cycle
cell cycle
multinucleation
D
% EdU positive cells
100
80
60
40
20
0
mock
vector
pRB
E
MyHC/DAPI
control 1
control 2
Rb1 shRNA
Rb1 shRNA
Kdm5a shRNA
F
% MyHC positive >2 nuclei cells
25
20
15
10
5
0
control 1
control 2
Rb1
Rb1 Kdm5a
G
control 1
control 2
Rb1 shRNA
Rb1 shRNA
Kdm5a shRNA
Kdm5a
pRb
MyHC
Mfn2
vinculin
H
size fractionation
pure myotubes
Poly(A)-RNA
RNA sequencing
Before fractionation
After fractionation
After fractionation
DAPI stained (4x ZOOM)

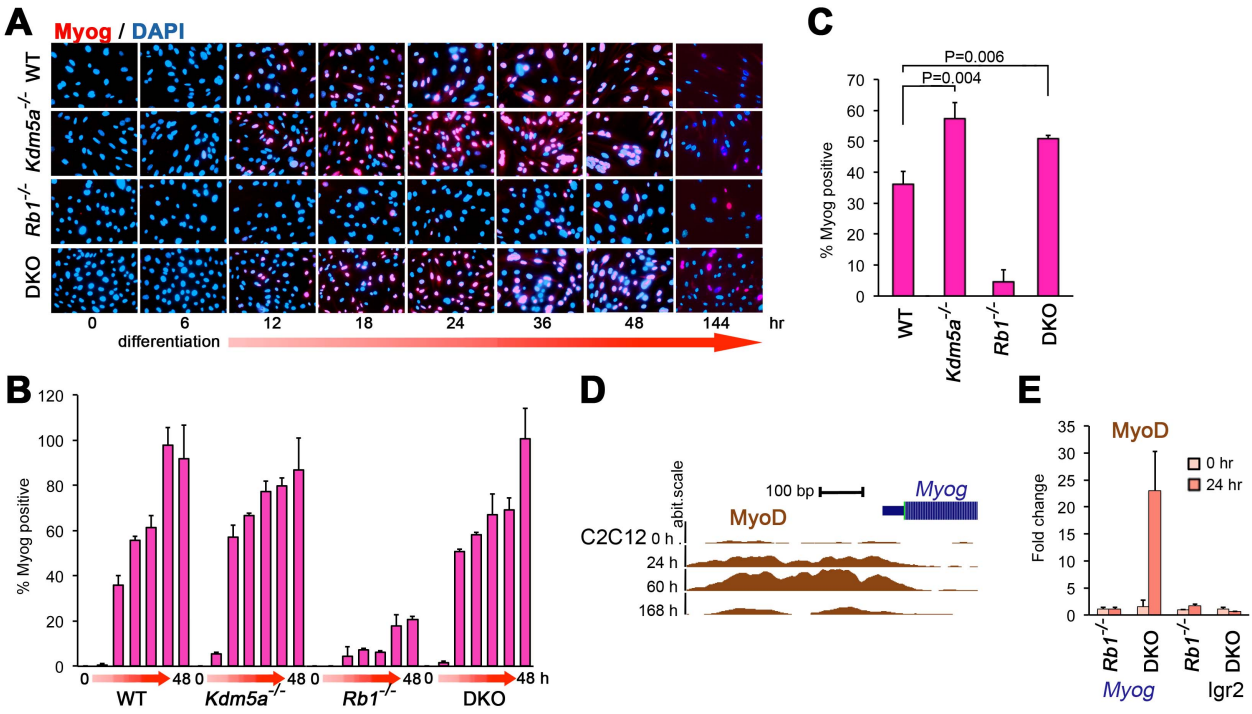
A
Myog / DAPI
WT
Kdm5a-/-
Rb1-/-
DKO
0
6
12
18
24
36
48
144
hr
differentiation
B
% Myog positive
WT
Kdm5a-/-
Rb1-/-
DKO
48 h
C
P=0.006
P=0.004
% Myog positive
D
C2C12
0 h
24 h
60 h
168 h
100 bp
Myog
MyoD
E
MyoD
0 hr
24 hr
Fold change
Myog
Igr2

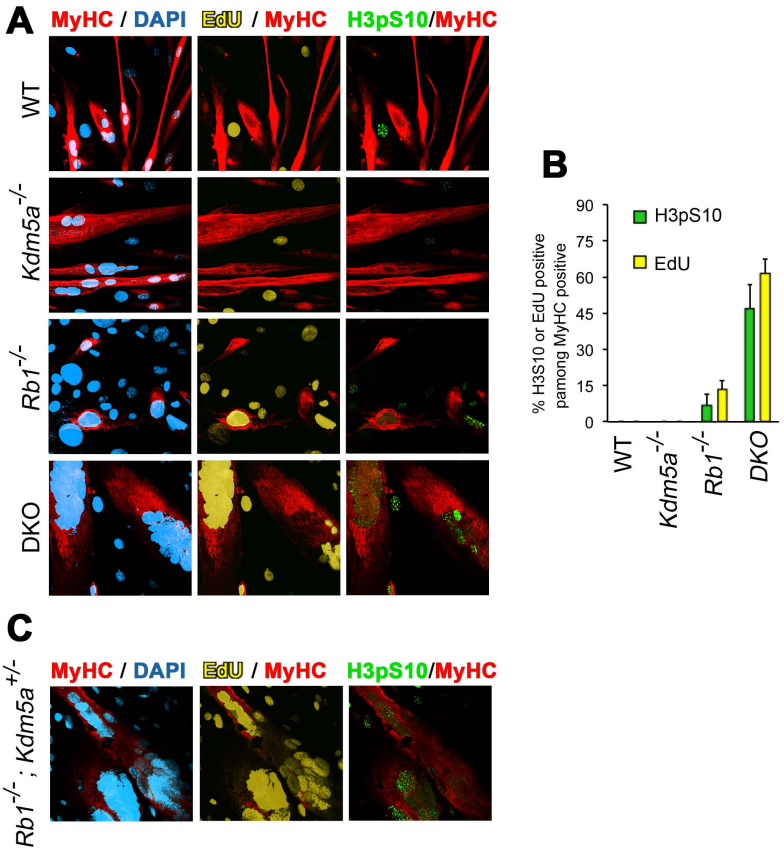
A
MyHC / DAPI
EdU / MyHC
H3pS10/MyHC
WT
Kdm5a-/-
Rb1-/-
DKO
B
H3pS10
EdU
% H3S10 or EdU positive pamong MyHC positive
90
75
60
45
30
15
0
WT
Kdm5a-/-
Rb1-/-
DKO
C
MyHC / DAPI
EdU / MyHC
H3pS10/MyHC
Rb1-/-; Kdm5a+/-

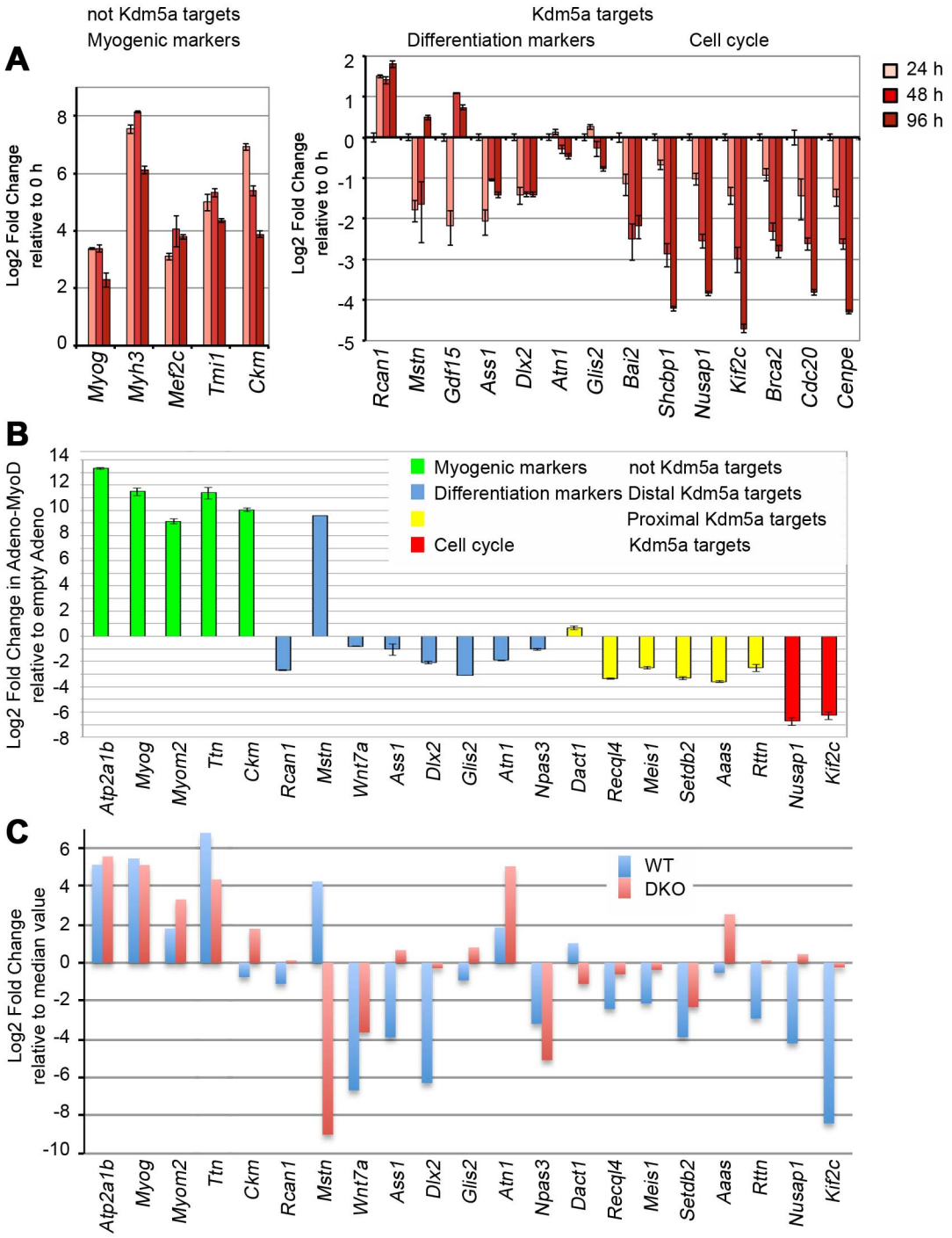
A
not Kdm5a targets
Myogenic markers
Kdm5a targets
Differentiation markers
Cell cycle
Log2 Fold Change relative to 0 h
24 h
48 h
96 h
Myog
Myh3
Mef2c
Tmi1
Ckm
Rcan1
Mstn
Gdf15
Ass1
Dlx2
Atn1
Glis2
Bai2
Shcbp1
Nusap1
Kif2c
Brca2
Cdc20
Cenpe
B
Log2 Fold Change in Adeno-MyoD relative to empty Adeno
Myogenic markers
Differentiation markers
Cell cycle
not Kdm5a targets
Distal Kdm5a targets
Proximal Kdm5a targets
Kdm5a targets
Atp2a1b
Myog
Myom2
Ttn
Ckm
Rcan1
Mstn
Wnt7a
Ass1
Dlx2
Glis2
Atn1
Npas3
Dact1
Recql4
Meis1
Setdb2
Aaas
Rttn
Nusap1
Kif2c
C
Log2 Fold Change relative to median value
WT
DKO
Atp2a1b
Myog
Myom2
Ttn
Ckm
Rcan1
Mstn
Wnt7a
Ass1
Dlx2
Glis2
Atn1
Npas3
Dact1
Recql4
Meis1
Setdb2
Aaas
Rttn
Nusap1
Kif2c

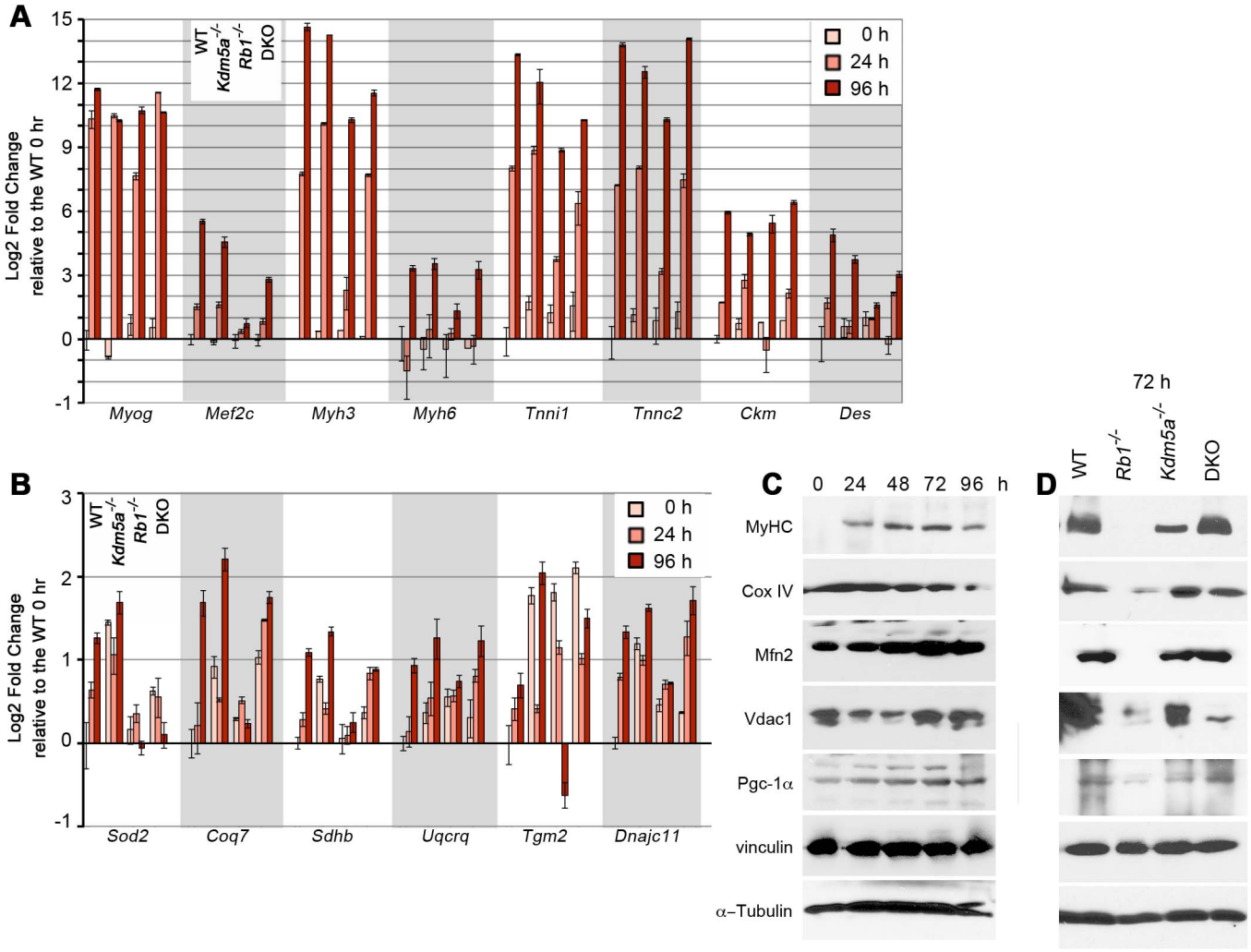
A
B
C
D
WT
Kdm5a-/-
Rb1-/-
DKO
0 h
24 h
96 h
Log2 Fold Change relative to the WT 0 hr
Myog
Mef2c
Myh3
Myh6
Tnni1
Tnnc2
Ckm
Des
Sod2
Coq7
Sdhb
Uqcrq
Tgm2
Dnajc11
0 24 48 72 96 h
MyHC
Cox IV
Mfn2
Vdac1
Pgc-1α
vinculin
α–Tubulin
72 h

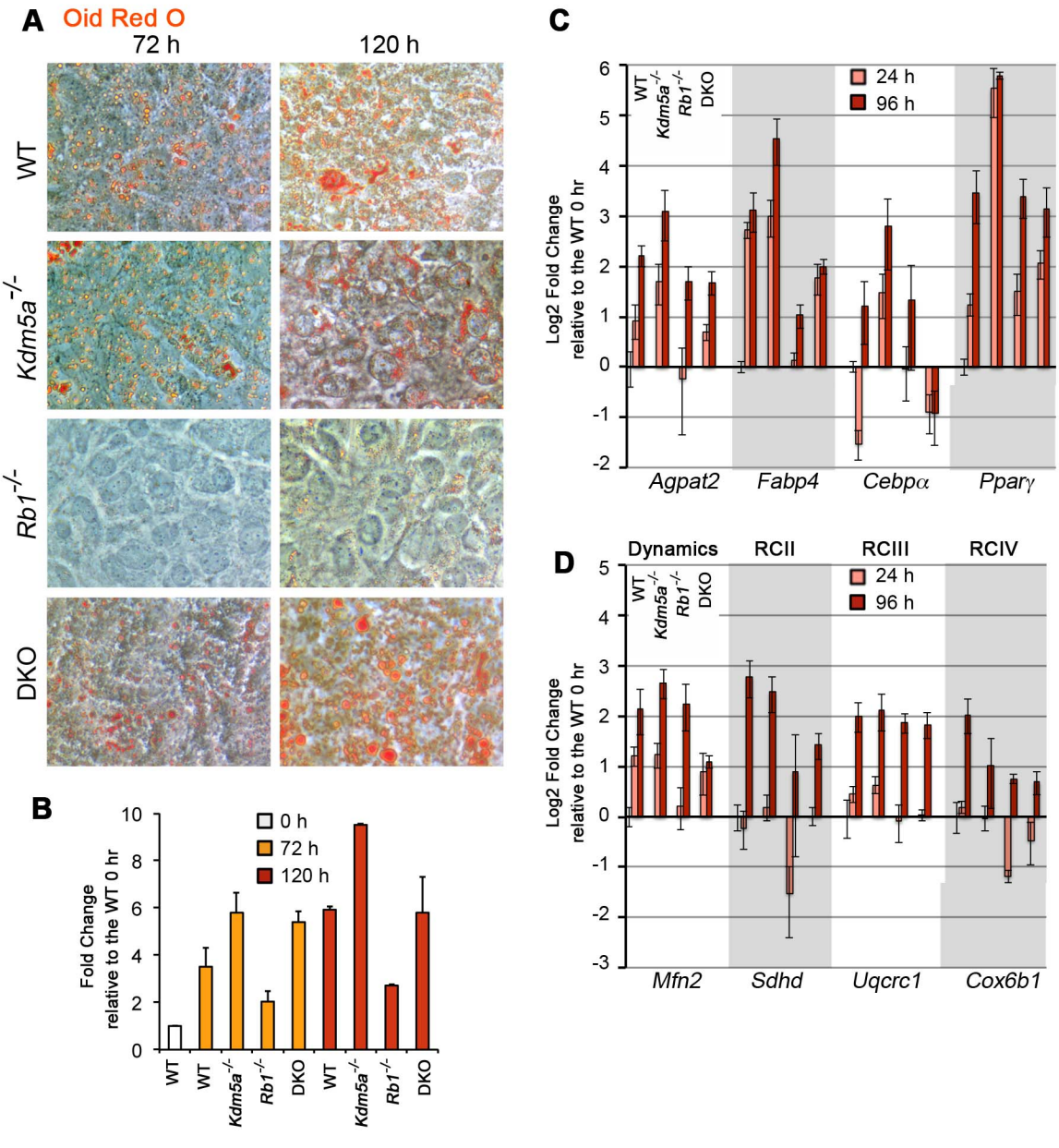
A
Oid Red O
72 h
120 h
WT
Kdm5a-/-
Rb1-/-
DKO
B
0 h
72 h
120 h
Fold Change relative to the WT 0 hr
WT
WT
Kdm5a-/-
Rb1-/-
DKO
WT
Kdm5a-/-
Rb1-/-
DKO
C
WT
Kdm5a-/-
Rb1-/-
DKO
24 h
96 h
Log2 Fold Change relative to the WT 0 hr
Agpat2
Fabp4
Cebpα
Pparγ
D
Dynamics
RCII
RCIII
RCIV
WT
Kdm5a-/-
Rb1-/-
DKO
24 h
96 h
Log2 Fold Change relative to the WT 0 hr
Mfn2
Sdhd
Uqcrc1
Cox6b1

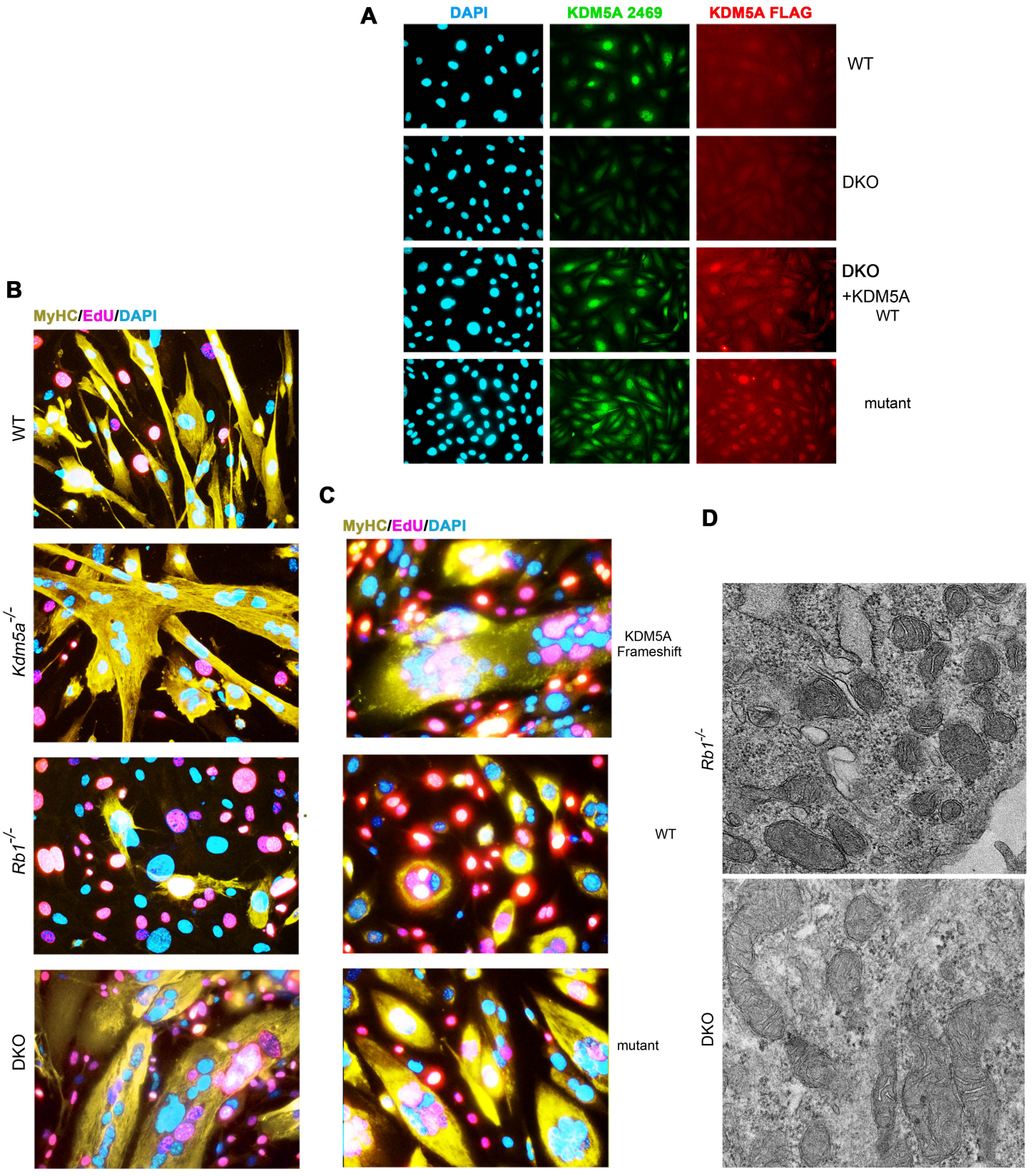
A
DAPI
KDM5A 2469
KDM5A FLAG
WT
DKO
DKO
+KDM5A
WT
mutant
B
MyHC/EdU/DAPI
WT
Kdm5a-/-
Rb1-/-
DKO
C
MyHC/EdU/DAPI
KDM5A
Frameshift
WT
mutant
D
Rb1-/-
DKO

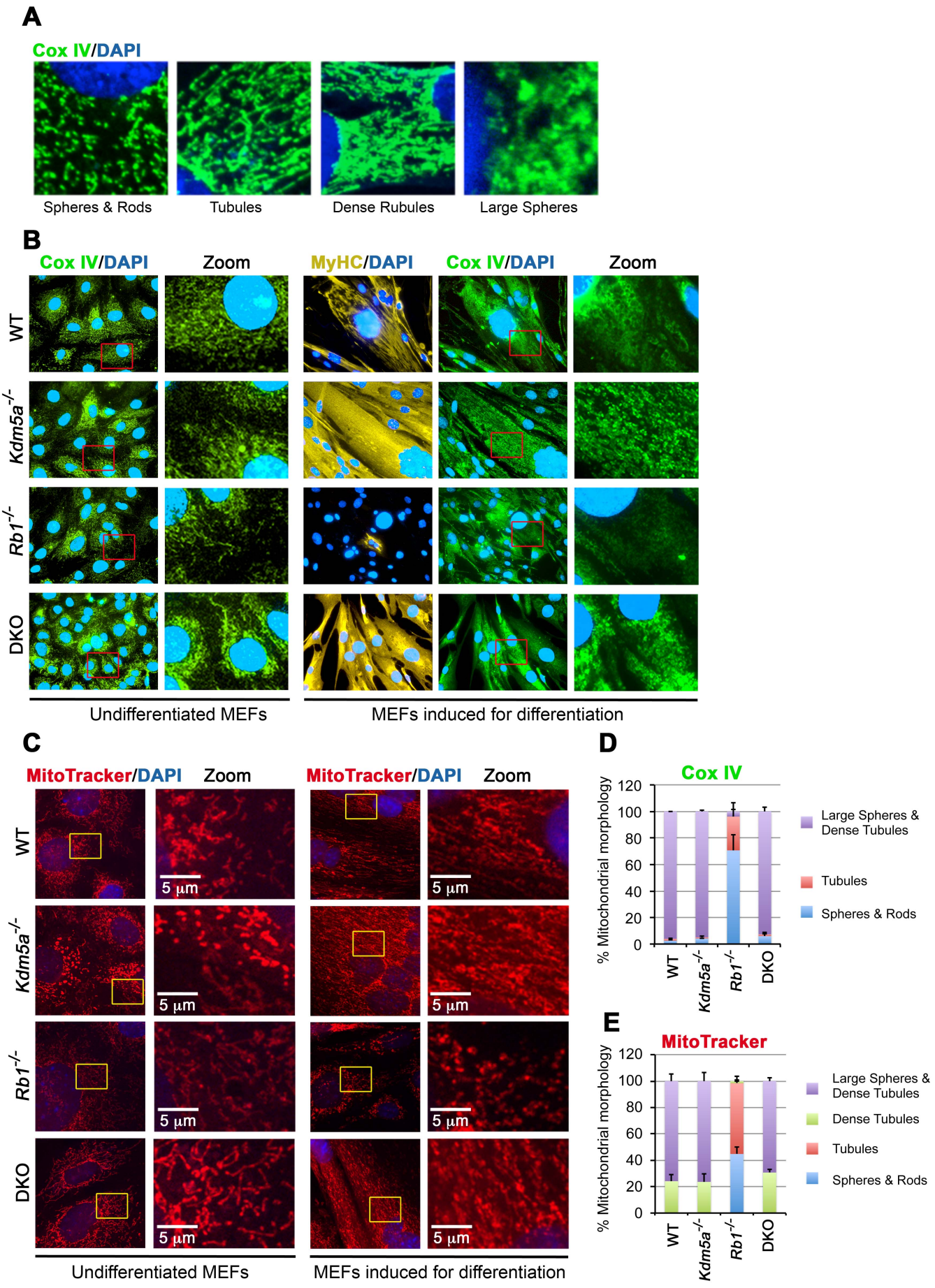
A
Cox IV/DAPI
Spheres & Rods
Tubules
Dense Rubules
Large Spheres
B
Cox IV/DAPI
Zoom
MyHC/DAPI
Cox IV/DAPI
Zoom
WT
Kdm5a-/-
Rb1-/-
DKO
Undifferentiated MEFs
MEFs induced for differentiation
C
MitoTracker/DAPI
Zoom
MitoTracker/DAPI
Zoom
5 µm
WT
Kdm5a-/-
Rb1-/-
DKO
Undifferentiated MEFs
MEFs induced for differentiation
D
Cox IV
% Mitochondrial morphology
120
100
80
60
40
20
0
WT
Kdm5a-/-
Rb1-/-
DKO
Large Spheres & Dense Tubules
Tubules
Spheres & Rods
E
MitoTracker
% Mitochondrial morphology
120
100
80
60
40
20
0
WT
Kdm5a-/-
Rb1-/-
DKO
Large Spheres & Dense Tubules
Dense Tubules
Tubules
Spheres & Rods

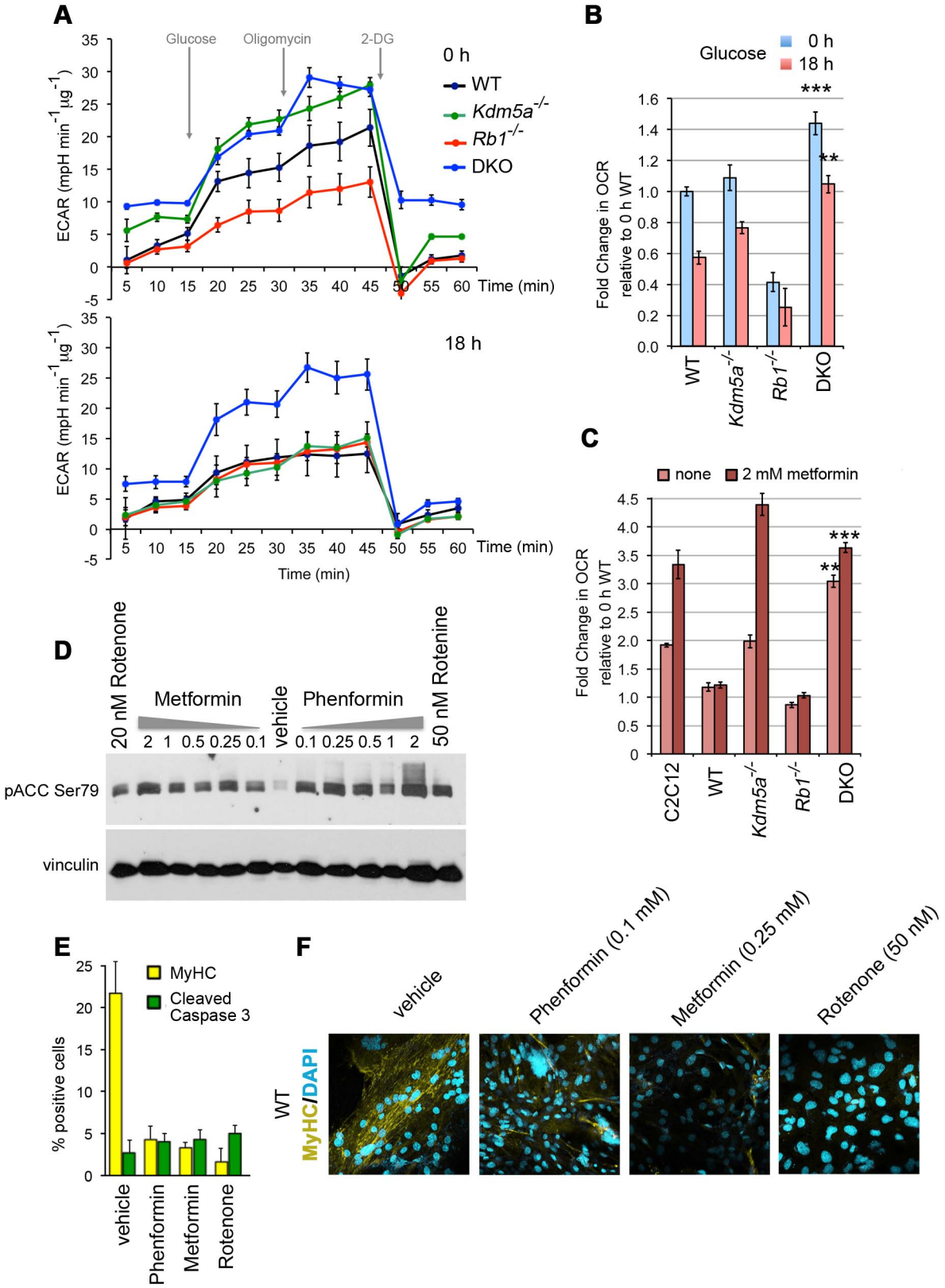
A
Glucose
Oligomycin
2-DG
0 h
WT
Kdm5a-/-
Rb1-/-
DKO
ECAR (mpH min-1 µg-1)
Time (min)
18 h
B
Glucose
0 h
18 h
Fold Change in OCR relative to 0 h WT
WT
Kdm5a-/-
Rb1-/-
DKO
C
none
2 mM metformin
Fold Change in OCR relative to 0 h WT
C2C12
WT
Kdm5a-/-
Rb1-/-
DKO
D
20 nM Rotenone
Metformin
vehicle
Phenformin
50 nM Rotenine
pACC Ser79
vinculin
E
MyHC
Cleaved Caspase 3
% positive cells
vehicle
Phenformin
Metformin
Rotenone
F
vehicle
Phenformin (0.1 mM)
Metformin (0.25 mM)
Rotenone (50 nM)
WT
MyHC/DAPI

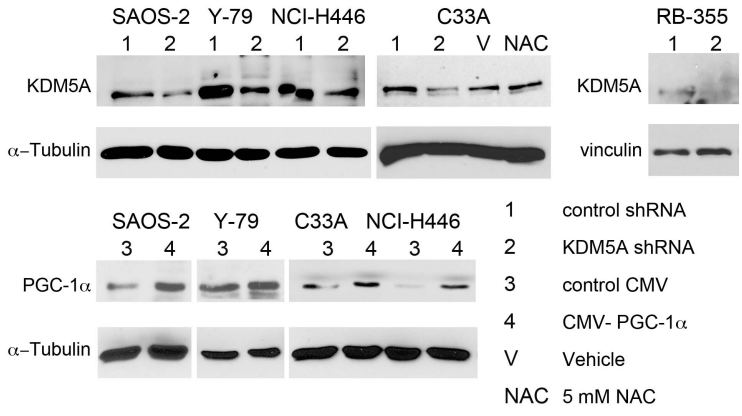
SAOS-2
Y-79
NCI-H446
C33A
RB-355
1 2 1 2 1 2 1 2 V NAC
1 2
KDM5A
α–Tubulin
KDM5A
vinculin
SAOS-2
Y-79
C33A
NCI-H446
3 4 3 4 3 4 3 4
PGC-1α
α–Tubulin
1 control shRNA
2 KDM5A shRNA
3 control CMV
4 CMV- PGC-1α
V Vehicle
NAC 5 mM NAC